

## Simulation Study of Seemingly Fickian but Heterogeneous Dynamics of Two Dimensional Colloids

Jeongmin Kim,<sup>1</sup> Chanjoong Kim,<sup>2</sup> and Bong June Sung<sup>1</sup>

<sup>1</sup>*Department of Chemistry, Sogang University, Seoul 121-742, Republic of Korea*

<sup>2</sup>*Chemical Physics Interdisciplinary Program and Liquid Crystal Institute, Kent State University, Kent, OH 44242, USA*  
(Received 4 October 2012; revised manuscript received 19 November 2012; published 24 January 2013)

A two-dimensional (2D) solid lacks long-range positional order and is diffusive by means of the cooperative motion of particles. We find from molecular dynamics simulations of hard discs that 2D colloids in solid and hexatic phases show seemingly Fickian but strongly heterogeneous dynamics. Beyond translational relaxation time, the mean-square displacement is linear with time,  $t$ , implying that discs would undergo Brownian diffusion and the self-part of the van Hove correlation function [ $G_s(r, t)$ ] might be Gaussian. But dynamics is still heterogeneous and  $G_s(r, t)$  is exponential at large  $r$  and oscillatory with multiple peaks at intermediate length. We attribute the existence of several such peaks to the observation that there are several clusters of discs with discretized mobility. The cluster of marginally mobile discs grows with time and begins to percolate around translational relaxation time while clusters of fast discs emerge in the middle of the marginally mobile cluster.

DOI: [10.1103/PhysRevLett.110.047801](https://doi.org/10.1103/PhysRevLett.110.047801)

PACS numbers: 61.20.Lc, 05.40.-a, 64.70.dj, 66.30.-h

Dynamics in supercooled liquids [1–3], gels [4], and porous materials [5] is complex and depends on both time and length scales. Three well-defined regimes of dynamics have been proposed based on simulations and experiments [6,7]. At short time and length scales, a ballistic motion is a dominant mechanism for diffusion. At very large spatiotemporal scales beyond translational relaxation time ( $\tau_\alpha$ ), the distribution of the particle displacement [the self-part of the van Hove correlation function,  $G_s(r, t)$ ] is Gaussian and the dynamics is Fickian; i.e., the mean-square displacement (MSD) is linear with time  $t$ . At an intermediate scale, particles may show subdiffusive behavior with  $\text{MSD} \sim t^b$  and  $b < 1$ .  $G_s(r, t)$  is not Gaussian and often divides into two parts that fit well with a Gaussian function for small  $r$  and an exponential function for large  $r$ , respectively [8]. And  $P(r, t)$  [ $\equiv 2\pi r G_s(r, t)$ ] often shows the second peak due to mobile particles that undergo hopping motions [9,10]. It has been supposed for decades that such a non-Gaussian  $G_s(r, t)$  would result in a non-Fickian diffusion at corresponding time scales. However, recent studies revealed that  $G_s(r, t)$  could be exponential instead of being Gaussian while Fickian diffusion is still observed with  $\text{MSD} \sim t$  [8,9,11]. In such cases, intermediate and large spatiotemporal scales are not always separated sharply; for example, Wang *et al.* showed that colloid beads on phospholipid bilayer tubes or in entangled actin suspensions entered the regime of Fickian diffusion while  $G_s(r, t)$  is non-Gaussian with an exponential tail at large  $r$  [11]. They suggested that Fickian diffusion with such a non-Gaussian distribution could be observed in various complex physicochemical and socioeconomic systems.

In this Letter, we report an important case of two-dimensional (2D) colloids where dynamics becomes

Fickian soon after  $\tau_\alpha$ , even though  $G_s(r, t)$  at intermediate length is neither Gaussian nor exponential but has several peaks for  $t \approx 12\tau_\alpha$ . We show that even in a simple system of 2D colloids the separation of intermediate and large spatiotemporal scales is unclear even after more than an order of magnitude times  $\tau_\alpha$ . This implies that 2D colloids in solid and hexatic phases undergo exceptionally correlated and collective motions. We also find that in a liquid phase, a caging time ( $\tau_c$ ), during which a particle is in a cage of neighbor particles before it escapes, is smaller than a noncaging time ( $\tau_{nc}$ ) that a particle has to wait before a cage forms to trap the particle. Near freezing transition,  $\tau_c \approx \tau_{nc}$ . Cage formation and hopping motion are sensitive to the thermodynamic phase transition.

2D solids might look as if they are simpler than 3D systems. However, due to the lack of a thermodynamically stable crystal and a long-range positional order in a solid phase [12], their dynamics is quite complex as well. According to the celebrated Kosterlitz-Thouless-Halperin-Nelson-Young theory, 2D solids would melt via an intermediate phase called a hexatic phase that does not exist in three-dimensional solids [13–15]. This has drawn great attention regarding the existence of the hexatic phase and the nature of transitions among solid, hexatic and liquid phases. A recent simulation study by Bernard and Krauth showed that the hexatic-to-solid transition was continuous and the hexatic-to-liquid transition was a first order phase transition [16]. There were relatively few studies on the 2D colloid dynamics near the melting transition [17]. Zangi and Rice found from a simulation study for a quasi-two-dimensional liquid that dynamics became strongly heterogeneous and the cooperative motions of particles were generated by instantaneous normal mode vibrations [18]. And dynamic criteria were introduced to identify 2D

melting transitions including a modified Lindemann parameter in 2D and the bond-angular correlation functions [19,20].

We model 2D colloids as hard discs of diameter  $\sigma$  that is the unit of length in this study. Initial configurations are obtained by placing discs in a square lattice randomly without any overlap between discs. The dimension  $L$  of a simulation cell is varied from 50 to 100 and periodic boundary conditions are applied in all directions. Initial configurations are equilibrated by performing discontinuous molecular dynamics (DMD) simulations. The mean-square displacement  $\langle \Delta r^2(t) \rangle = \langle |\vec{r}(t) - \vec{r}(0)|^2 \rangle$  and the self-part of the van Hove correlation function  $G_s(r, t) = \langle \delta\{\vec{r} - [\vec{r}(t) - \vec{r}(0)]\} \rangle$  are estimated using equilibrated configurations from DMD simulations [6]. Here,  $\langle \cdot \cdot \rangle$  denotes an ensemble average and  $\vec{r}(t)$  is the position vector of a disc at time  $t$ . We also monitor the self-part of the intermediate scattering function  $F_s(k, t) = \langle \exp\{ik \cdot [\vec{r}(t) - \vec{r}(0)]\} \rangle$  and a 2D non-Gaussian parameter,  $\alpha_2(t) \equiv 1/2 \langle \Delta r^4(t) \rangle / \langle \Delta r^2(t) \rangle^2 - 1$ .  $F_s(k, t)$  is the spatial Fourier transform of  $G_s(r, t)$  and provides information on spatio-temporal correlations of particles.

The area fraction of hard discs ( $\phi = \frac{\pi\sigma^2 N}{4L^2}$ ) ranges from 0.66 to 0.76, which covers liquid, hexatic and solid phases.  $N$  denotes the number of discs in the system. According to Bernard and Krauth, the hexatic-to-solid phase transition occurs at  $\phi = 0.720$ , a single-phase hexatic regime exists for  $0.716 < \phi < 0.720$ , and liquid and hexatic phases coexist for  $0.7 < \phi < 0.716$  [16]. Because of our relatively

small system size, it is difficult to pinpoint exact phase boundaries, but we identify all three phases. We calculate bond order correlation functions and find that its susceptibility diverges at  $\phi = 0.704$ , which indicates the freezing transition of 2D liquids [21,22]. Beyond  $\phi = 0.717$  the bond order correlation function starts showing a long range orientational order, which is a signature of the hexatic-to-solid phase transition. In order to confirm phase behaviors, we also investigate pair correlation functions and the snapshots of discs assigned with local orientation vectors [16,20,23].

Dynamics becomes heterogeneous in hexatic and solid phases. At short time scales, particles diffuse via ballistic motions with few collisions. Mean-square displacements ( $\langle \Delta r^2(t) \rangle$ ) overlap well with one another and scale as  $t^2$  [Fig. 1(a)]. At long time scales, particles enter the Fickian regime even in a solid phase with  $\langle \Delta r^2(t) \rangle \sim t$  because there is no long-range positional order in 2D solids. At intermediate scales in hexatic and solid phases,  $\langle \Delta r^2(t) \rangle$  shows a subdiffusive behavior, i.e.,  $\langle \Delta r^2(t) \rangle \sim t^b$  with  $b < 1$ . In a solid phase for  $\phi > 0.72$ , even a plateau appears in  $\langle \Delta r^2(t) \rangle$ . The intermediate regime becomes longer in time as  $\phi$  increases.

The 2D non-Gaussian parameter  $\alpha_2(t)$ , an indicator of the dynamic heterogeneity, shows clearly that dynamics is heterogeneous at intermediate scales in hexatic and solid phases [Fig. 1(b)].  $\alpha_2(t) \approx 0$  in a liquid phase, but  $\alpha_2(t)$  increases with  $\phi$ .  $\tau_{ng}$ , the time at which  $\alpha_2(t)$  reaches a maximum and dynamics is the most heterogeneous,

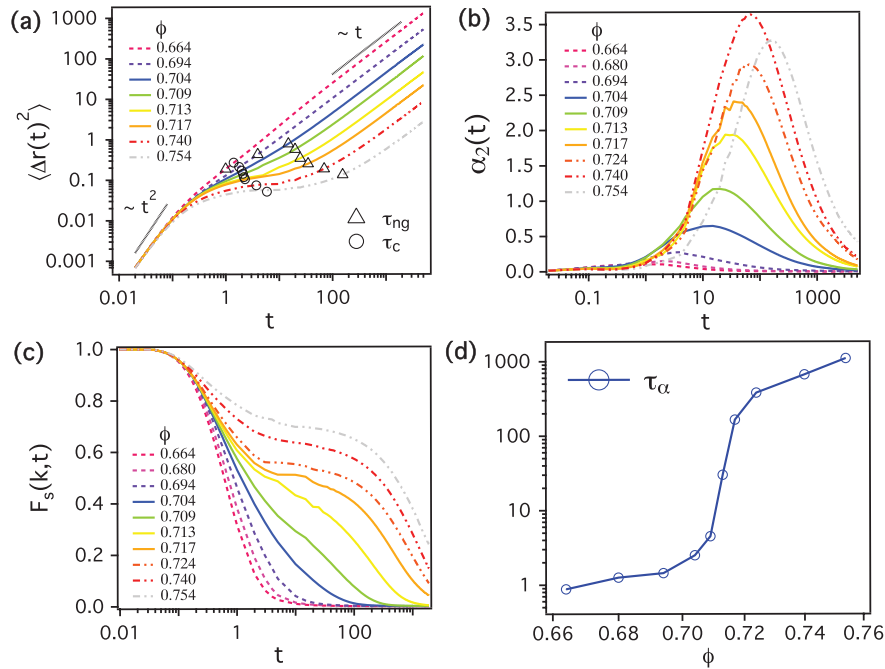


FIG. 1 (color). (a) Mean-square displacements [ $\langle \Delta r^2(t) \rangle$ ], (b) a 2D non-Gaussian parameter [ $\alpha_2(t)$ ], (c) the self part of the intermediate scattering function [ $F_s(k, t)$ ] with  $k = 6$ , and (d) the translational relaxation time ( $\tau_\alpha$ ). In Fig. 1,  $\tau_c$  and  $\tau_{ng}$  denote the caging time and the time at  $\alpha_2(t)$  is maximum, respectively.

increases monotonically with  $\phi$ . As shown in Fig. 1(a), around  $\tau_{ng}$  discs leave an intermediate regime for a Fickian regime.

Subdiffusive dynamic behaviors in hexatic and solid phases are reflected well in  $F_s(k, t)$  [Fig. 1(c)]. In hexatic and solid phases,  $F_s(k, t)$  is well fitted to a stretched exponential function called the *Kohlrausch-Williams-Watts* function, i.e.,  $F_s(k, t) \sim \exp\{(-t/\tau_\alpha)^\beta\}$  with  $0 < \beta \leq 1$  [7]. As  $\phi$  increases,  $F_s(k, t)$  decays more slowly with a plateau appearing and its height rising. An increase in the plateau height was also observed for a sol-gel transition and could be attributed to the structural changes [4]. The translational relaxation time  $\tau_\alpha$  is determined using a relation  $F_s(k=6, t=\tau_\alpha) = e^{-1}$ . As depicted in Fig. 1(d),  $\tau_\alpha$  does not change much in a liquid phase but increases sharply in a narrow region of a hexatic phase.

$\langle \Delta r^2(t) \rangle$  and  $F_s(k, t)$  indicate that systems should enter a Fickian regime soon after  $\tau_\alpha$  (or  $\tau_{ng}$ ). This implies that at long time scales, spatiotemporal correlations of particles would be lost and the particle displacement would become Gaussian, which is, however, not the case in the hexatic and solid phases of 2D colloids. As depicted in Figs. 2(b) and 2(d), the self-part of the van Hove correlation function  $G_s(r, t)$  is not Gaussian and  $P(r, t) [= 2\pi r G_s(r, t)]$  shows several peaks. For  $\phi = 0.717$   $\langle \Delta r^2(t) \rangle \sim t$  for  $t \geq 100$  and  $F_s(k=6, t)$  decays most thoroughly at  $t = 1000$ . But  $G_s(r, t)$  is still not Gaussian until  $t = 1990$  even with six peaks in  $P(r, t)$ . Note that  $t = 1990$  corresponds  $12\tau_\alpha$ . Non-Gaussian  $G_s(r, t)$  with several peaks persists even for  $t = 12\tau_\alpha$  while  $\langle \Delta r^2(t) \rangle$  enters the Fickian regime

and  $F_s(k, t)$  decays at  $t > \tau_\alpha$ . Therefore, this 2D colloid near the hexatic-to-solid transition is a clear example that non-Gaussian particle displacements still result in seemingly Fickian dynamics. For  $\phi = 0.713$  in a hexatic phase [Fig. 2(a)], peaks in  $P(r, t)$  disappear after  $t = 1000$ . Even though  $P(r, t)$  does not have peaks at  $t = 1990$ ,  $G_s(r, t)$  fits to a Gaussian function only at small  $r$  and fits to exponential functions at large  $r$ . The exponential distribution of particle displacement was also observed in glasses, gels, and entangled actin suspensions [4,11,24].

The peaks in  $P(r, t)$  are located around the integral multiples of the disc diameter, which implies that discs should diffuse via stringlike collective hopping motions [18]. Figure 2(c) depicts a representative trajectory of a disc for  $\phi = 0.717$ . The disc undergoes almost 5 times the discretized hopping motions in  $6\tau_\alpha$ . Zangi and Rice suggested that the collective motion should be generated by superpositions of instantaneous normal mode vibrations and their lifetimes should increase with  $\phi$  [18,25,26].

The existence of the multiple peaks in  $P(r, t)$  at intermediate length can be understood by looking at how clusters of mobile particles form and grow. Figure 3 shows simulation snapshots of a trajectory for  $\phi = 0.717$  at four particular times. A color code is assigned to each disc according to a maximum displacement  $[\mu_i(t^*)]$  of the disc in a given time, i.e.,  $\mu_i(t^*) = \max(|\vec{r}(t_2) - \vec{r}(t_1)|)$  for  $t_0 \leq t_1 < t_2 \leq t_0 + t^*$ . For example, yellow discs travel up to a discretized distance of  $5\sigma$  during a given time. And grey discs rattle around their positions, traveling less than  $1\sigma$ . Two discs are determined to be connected if

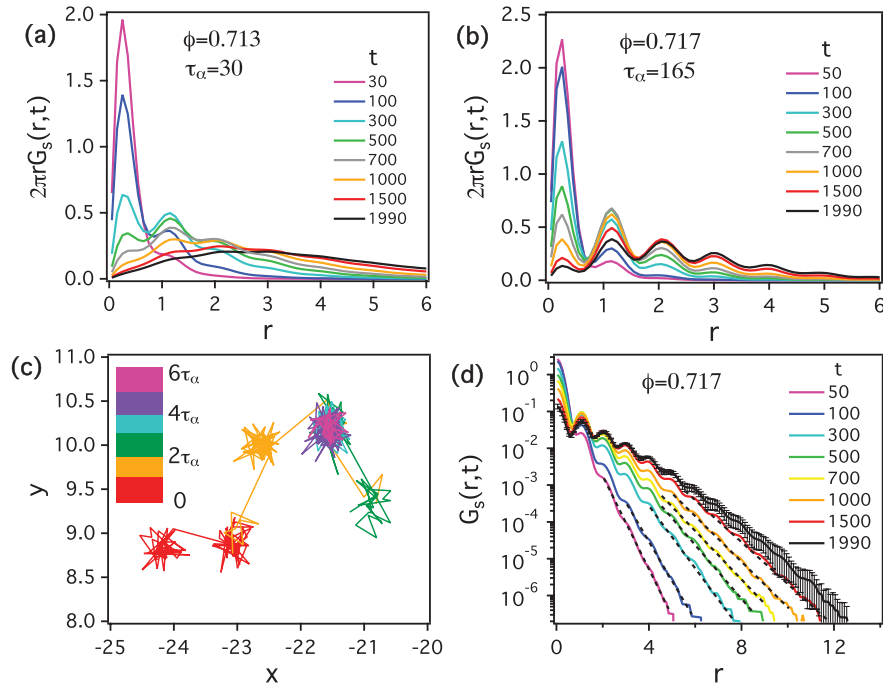


FIG. 2 (color).  $2\pi r G_s(r, t)$  for (a)  $\phi = 0.713$  and (b)  $\phi = 0.717$ . (c) A representative trajectory of a disc for  $\phi = 0.717$  that undergoes hopping motions 5 times in  $6\tau_\alpha$ . Different colors indicate different times divided into 6  $\tau_\alpha$ 's. (d)  $G_s(r, t)$  for  $\phi = 0.717$ . Dashed lines are fits to exponential functions.

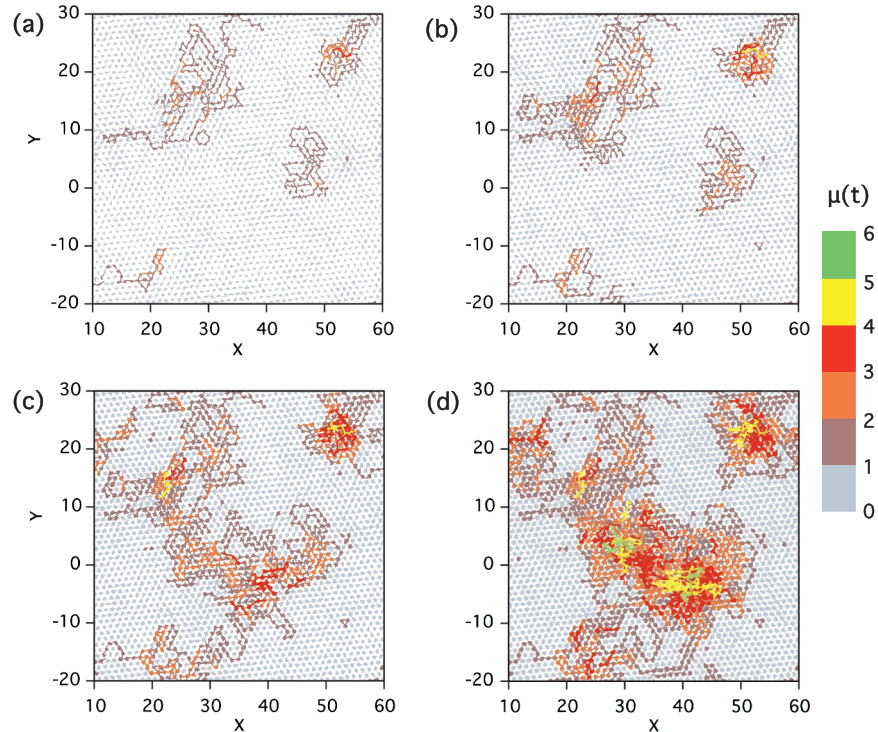


FIG. 3 (color). Snapshots of a representative trajectory for  $\phi = 0.717$  and 4 different times (a)  $t = \tau_\alpha/4$ , (b)  $\tau_\alpha/2$ , (c)  $\tau_\alpha$ , and (d)  $2\tau_\alpha$ . The color code of discs is determined based on the maximum displacement of each disc in a given time.

their colors are the same and they are the nearest neighbor of each other. A cluster is defined as a set of discs that are connected via at least one path. Therefore, discs in a cluster possess almost the same mobility at a given time and diffuse collectively.

At  $t = \tau_\alpha/4$  [Fig. 3(a)], most discs travel less than  $\sigma$ . However, there are four brown clusters of marginally mobile discs that travel more than  $\sigma$  but less than  $2\sigma$ . When  $t = \tau_\alpha/2$  [Fig. 3(b)], the four brown clusters grow. New orange or red clusters of discs with higher mobility, which travel more than  $2\sigma$ , emerge in the middle of a brown cluster. The new cluster with higher mobility is more or less enclosed with a large cluster with lower mobility. For  $t = \tau_\alpha$ , the brown clusters begin to percolate

a simulation cell while more mobile but smaller clusters keep growing. As depicted in Fig. 3(d), new faster (yellow or green) clusters keep emerging in the middle of the original slower clusters. Two clusters of green discs that travel even up to  $6\sigma$  appear. And layers of clusters of discretized mobility are observed clearly. Each cluster accounts for the peak of  $P(r, t)$ . Some discs diffuse through a percolating path of mobile clusters. However, many other grey discs are still frozen at the place where those discs were located initially at  $t = 0$ . Therefore, dynamics should be spatially heterogeneous even at  $t > \tau_\alpha$ .

The cluster size grows with time as depicted in Fig. 4(a). The cluster size ( $\sqrt{N_C}$ ) is defined as the square-root of the number of all discs surrounded by the largest brown cluster

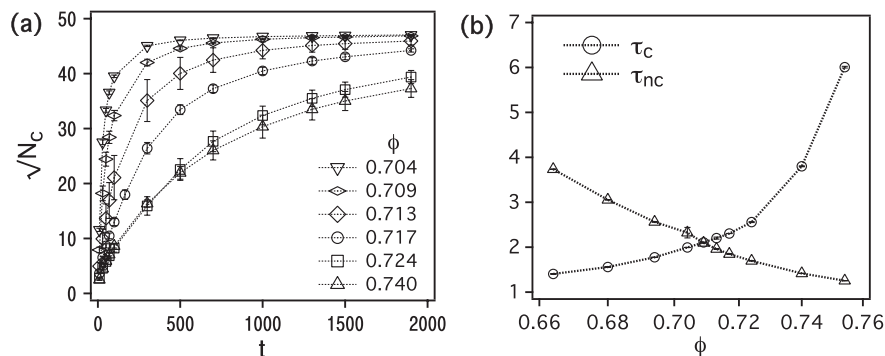


FIG. 4. (a) The size of clusters ( $\sqrt{N_C}$ ) of mobile regions as a function of time and (b) caging time,  $\tau_c$  and noncaging time,  $\tau_{nc}$  as a function of  $\phi$ .



in a simulation cell [27,28]. After a certain time for a given value of  $\phi$ ,  $\sqrt{N_C}$  reaches a plateau because the largest cluster begins to percolate and most discs in a simulation cell belong to the cluster. For a smaller  $\phi$ , due to a faster diffusion,  $\sqrt{N_C}$  reaches a plateau earlier.

Two characteristic times are calculated to investigate hopping motions and the formation and the breakdown of a cage that confine a disc. A cage is defined as follows. We perform Voronoi tessellation and find a first shell of neighbor discs around a particular disc. Then, if the center of the disc is located within a triangle made of any pair of three neighbor discs and all sides of the triangle is smaller than  $2\sigma$ , we decide that a cage forms and the disc is trapped within the cage [20]. A caging time ( $\tau_c$ ) is an average time taken for a disc to spend before hopping out of the cage. A noncaging time ( $\tau_{nc}$ ) is defined as an average time for a disc to wait before a cage forms and starts trapping the disc.

At small spatiotemporal scales, hopping motions are quite sensitive to the thermodynamic phase transition of 2D colloids.  $\tau_c$  and  $\tau_{nc}$  are much smaller than  $\tau_\alpha$ , which suggests that hopping motions do not occur every time cages break down and form, but with much less chance. This is because even though a cage breaks, a disc has to translate in an appropriate direction at the moment in order to escape the cage. In a liquid phase,  $\tau_{nc}$  is larger than  $\tau_c$ . Therefore, a disc is less likely to be trapped in a cage. And even though a cage forms and traps a disc, it would not take a long time for the disc to escape. But in hexatic and solid phases,  $\tau_c$  is larger than  $\tau_{nc}$ , which means that discs are likely to be trapped in a cage. Plateaus of  $\langle \Delta r^2(t) \rangle$  for discs in solid phases are observed at the same time scales of  $\tau_c$  [Fig. 1(a)]. Because  $\tau_c$  increases and  $\tau_{nc}$  decreases with an increase in  $\phi$ , they cross at a certain value of  $\phi$  near the liquid-to-hexatic phase transition.

In summary, we perform DMD simulations to investigate the dynamics of 2D colloids near melting transitions. The mean-square displacement and the self-part of intermediate scattering functions suggest that the dynamics enters a Fickian regime around the translational relaxation time. This often implies that the particle displacement distribution might be Gaussian beyond the translational relaxation time. We find, however, that near melting transition, the self-part [ $G_s(r, t)$ ] of the van-Hove correlation function is not Gaussian with oscillatory multiple peaks at intermediate length for long times until  $12\tau_\alpha$ . Unlike in gels and supercooled liquids,  $G_s(r, t)$  is neither Gaussian nor exponential at intermediate values of  $r$ , but has several peaks that persist for  $12\tau_\alpha$  in solid phases. We illustrate that such peaks appear because the mobility of dynamics clusters is more or less discretized. At short spatiotemporal scales, the formation and the breakdown of cages are sensitive to the phase transition of 2D colloids. Caging time ( $\tau_c$ ) increases and noncaging time ( $\tau_{nc}$ ) decreases with an increase of  $\phi$ . They become equal to each other around the liquid-to-hexatic phase transition.

This work was supported by the National Research Foundation of Korea (NRF) under Grant No. NRF-2011-220-C00030. This research was supported by the Global Frontier Research Program (2011-0032155) and Advanced Research Center for Nuclear Excellence funded by MEST, Korea.

- 
- [1] M. D. Ediger, *Annu. Rev. Phys. Chem.* **51**, 99 (2000).
  - [2] W. K. Kegel and A. van Blaaderen, *Science* **287**, 290 (2000).
  - [3] E. R. Weeks, J. C. Crocker, A. C. Levitt, A. Schofield, and D. A. Weitz, *Science* **287**, 627 (2000).
  - [4] P. I. Hurtado, L. Berthier, and W. Kob, *Phys. Rev. Lett.* **98**, 135503 (2007).
  - [5] J. Kurzidim, D. Coslovich, and G. Kahl, *Phys. Rev. E* **82**, 041505 (2010).
  - [6] J. Hansen and I. McDonald, *Theory of Simple Liquids* (Elsevier Academic Press, London, 2006).
  - [7] L. Berthier, G. Biroli, J. Bouchaud, L. Cipelletti, and W. van Saarloos, *Dynamical Heterogeneities in Glasses, Colloids, and Granular Media* (Oxford University Press, Oxford, 2011).
  - [8] B. Wang, J. Kuo, S. C. Bae, and S. Granick, *Nat. Mater.* **11**, 481 (2012).
  - [9] G. Szamel and E. Flenner, *Phys. Rev. E* **73**, 011504 (2006).
  - [10] Th. Voigtmann and J. Horbach, *Phys. Rev. Lett.* **103**, 205901 (2009).
  - [11] B. Wang, S. M. Anthony, S. C. Bae, and S. Granick, *Proc. Natl. Acad. Sci. U.S.A.* **106**, 15160 (2009).
  - [12] N. D. Mermin, *Phys. Rev.* **176**, 250 (1968).
  - [13] J. M. Kosterlitz and D. J. Thouless, *J. Phys. C* **6**, 1181 (1973).
  - [14] B. I. Halperin and D. R. Nelson, *Phys. Rev. Lett.* **41**, 121 (1978).
  - [15] A. P. Young, *Phys. Rev. B* **19**, 1855 (1979).
  - [16] E. P. Bernard and W. Krauth, *Phys. Rev. Lett.* **107**, 155704 (2011).
  - [17] U. Gasser, *J. Phys. Condens. Matter* **21**, 203101 (2009).
  - [18] R. Zangi and S. A. Rice, *Phys. Rev. Lett.* **92**, 035502 (2004).
  - [19] K. Zahn and G. Maret, *Phys. Rev. Lett.* **85**, 3656 (2000).
  - [20] Z. Wang, A. M. Alsayed, A. G. Yodh, and Y. Han, *J. Chem. Phys.* **132**, 154501 (2010).
  - [21] K. Binder, S. Sengupta, and P. Nielaba, *J. Phys. Condens. Matter* **14**, 2323 (2002).
  - [22] H. Weber, D. Marx, and K. Binder, *Phys. Rev. B* **51**, 14636 (1995).
  - [23] T. M. Truskett, S. Torquato, S. Sastry, P. G. Debenedetti, and F. H. Stillinger, *Phys. Rev. E* **58**, 3083 (1998).
  - [24] P. Chaudhuri, L. Berthier, and W. Kob, *Phys. Rev. Lett.* **99**, 060604 (2007).
  - [25] M. Buchner, B. M. Ladanyi, and R. M. Stratt, *J. Chem. Phys.* **97**, 8522 (1992).
  - [26] S. A. Rice, *Phys. Rev.* **112**, 804 (1958).
  - [27] T. Kawasaki, T. Araki, and H. Tanaka, *Phys. Rev. Lett.* **99**, 215701 (2007).
  - [28] M. M. Hurley and P. Harrowell, *Phys. Rev. E* **52**, 1694 (1995).